

## RESEARCH ARTICLE

# Low Loss Multi-Channel Communication Combiner for Cellular Applications

ERAN ROSENBERG<sup>1</sup>, YOAV KORAL<sup>1</sup>, ACHIMEIR MEKEYESS<sup>1</sup>, MOSHE MIZRACHI<sup>1</sup>,  
DORON SOLOMON<sup>1</sup>, ELDAD HOLDENGREBER<sup>1,2</sup>, SHMUEL E. SCHACHAM<sup>1</sup>,  
AND ELIYAHU FARBER<sup>1,3</sup>

<sup>1</sup>Department of Electrical and Electronic Engineering, Ariel University, Ariel 40700, Israel

<sup>2</sup>Department of Mechanical Engineering and Mechatronics, Ariel University, Ariel 40700, Israel

<sup>3</sup>Department of Physics, Ariel University, Ariel 40700, Israel

Corresponding author: Eldad Holdengreber (eldadh@ariel.ac.il)

**ABSTRACT** The increasing demand for cellular communication channels calls for multichannel solutions. Using one antenna for each channel results in a high density of antennas at the compact cellular station front, which generates inter-channel interference. This may result in distractive interference and significant losses at the output and input of the channels. To overcome these drawbacks, we propose a technology that combines several channels into a single antenna. We implemented a frequency-tuned, multi-channel phase control system with a phase shifter connected to each channel, with low insertion loss and low return loss. The phase shifter is composed of an ultra-wideband coupler and a computer-controlled capacitor. To obtain low insertion loss of the phase shifter, typically 1.5 dB, we designed a planar tandem hybrid coupler for the desired frequency range. We used a capacitor bank of varactor diodes for frequency tuning. The capacitance of these diodes was controlled by the applied reverse bias voltage generated by a D/A converter. The control computer received the digital input to the converter through a serial communication line. The channels were simultaneously phase matched to minimize channel losses. We performed an extensive theoretical analysis of a multi-channel frequency combiner. Based on the simulation results, a three-channel multi-coupler was implemented. The high performance of the system was demonstrated experimentally.

**INDEX TERMS** Cellular communication, directional couplers, impedance matching, insertion loss, multi-channel antenna, phase shifters, wideband.


## I. INTRODUCTION

The advance of cellular communication requires increased communication channels per device or base station. Increasing the number of channels while allocating a separate antenna to every channel increases the device's volume, consuming precious volume. Moreover, a large number of antennas can lead to destructive interference between them.

One approach for reducing the number of antennas is combining several channels into one. However, without proper phase matching, this configuration may result in distractive interference and significant loss at the outputs and inputs of the channels. Several approaches are available for handling

matching problems, such as Triplexer [1], [2] or Combiner / Splitter [3], [4]. However, these solutions have drawbacks, such as being limited to fixed frequencies (Triplexer) or inherent high insertion loss (~6 dB in a three-channel combiner).

Multi-channel phase control systems for the UHF and VHF bands were developed to obtain a frequency-tuned, low insertion loss and low return loss matching unit [5], [6], [7]. These systems allow simultaneous transmission and reception of several channels through a single antenna, thereby reducing the number of antennas. We developed a high-performance phase shifter for the VHF band to reduce total system losses using High-Temperature Superconducting (HTSC) technology. A three-channel multi-coupler system was implemented with HTSC components [8], [9], [10]. To achieve phase matching, it is necessary to incorporate in the phase shifter

The associate editor coordinating the review of this manuscript and approving it for publication was Barbara Masini .

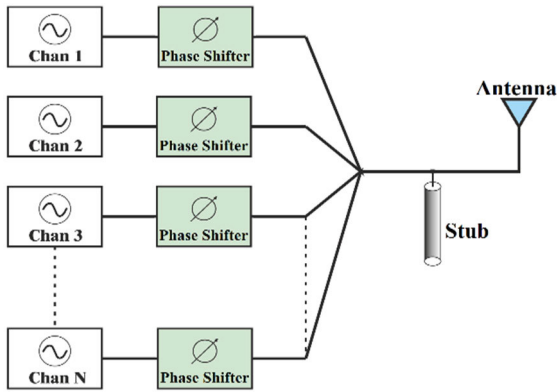


FIGURE 1. Multi-channel phase control system.



FIGURE 2. Phase shifter with a hybrid 90° coupler.

a specific capacitance adapted to the frequency combination of operation [11]. To that end, the system included switched capacitor banks [12], which enabled the user to change the frequency combination dynamically during operation. However, this technique increases insertion loss due to the switching elements' parasitic reactance and ohmic losses. This effect becomes much more significant at the higher frequencies of the cellular band [13].

To overcome the insertion loss problems, we introduced several technological improvements. We designed and implemented a state-of-the-art planar tandem hybrid coupler [14] for the desired frequency range. We replaced the switching capacitor bank with computer-controlled varactor diodes.

Additionally, we performed an extensive theoretical investigation of a multi-channel frequency combiner, presented in Section II. Based on the simulation results, a three-channel multi-coupler was implemented. The system's performance was measured, and the results are presented in Section III.

## II. MULTI-CHANNEL SYSTEM DESIGN

### A. SYSTEM CONFIGURATION

A schematic design of a multi-channel phase control system is shown in Fig. 1. It was designed for the frequency range of 0.8 GHz to 2.4 GHz.

By using varactor diodes instead of a switching capacitor bank for frequency selection, the estimated value of the insertion loss of the phase shifter is reduced from 3 dB to about 1.5 dB. In addition, we geared for S11 lower than -15 dB.

The proper way to comply with these specifications is to design the phase shifter with a hybrid 90° coupler (Fig. 2).

### B. SYSTEM EQUATIONS

The scattering matrix of the hybrid 90° coupler is given by [6]:

$$\begin{bmatrix} b_1 \\ b_2 \\ b_3 \\ b_4 \end{bmatrix} = \begin{bmatrix} 0 & C & T & 0 \\ C & 0 & 0 & T \\ T & 0 & 0 & C \\ 0 & T & C & 0 \end{bmatrix} \cdot \begin{bmatrix} a_1 \\ a_2 \\ a_3 \\ a_4 \end{bmatrix} \quad (1)$$

where C and T are the coupling and transmission coefficients.  $a$  and  $b$  are the normalized input and output wave vectors, respectively. Using the reflection coefficient of the varactor capacitance, given by

$$\Gamma_c = \frac{1/j\omega C - Z_0}{1/j\omega C + Z_0} = e^{-j2 \arctan(\omega Z_0 C)}, \quad (2)$$

the reflection coefficients relations at the ports of the coupler can be expressed as

$$a_2 = \Gamma_c b_2 ; \quad a_3 = \Gamma_c b_3 . \quad (3)$$

Introducing equations (3) into (1), we obtain the scattering matrix of the phase shifter,

$$\begin{bmatrix} b_1 \\ b_4 \end{bmatrix} = \begin{bmatrix} S_{11} & S_{21} \\ S_{21} & S_{22} \end{bmatrix} \cdot \begin{bmatrix} a_1 \\ a_4 \end{bmatrix} \quad (4)$$

where:

$$S_{11} = S_{22} = \Gamma_c (C^2 + T^2) ; \quad S_{21} = 2\Gamma_c CT . \quad (5)$$

The reflection coefficient  $\Gamma_{ij}$  of channel  $j$  at frequency  $\omega_i$  of channel  $i$ , as seen from the junction of the system, can be expressed as:

$$\Gamma_{ij} = \left\langle S_{11} + \frac{S_{21}^2 \Gamma_B}{1 - S_{22} \Gamma_B} \right\rangle_{ij} \quad (6)$$

where  $\Gamma_B$  is the out-of-band reflection coefficient of each Band Pass Filter (BPF).  $\Gamma_B$  is typically about -1. The admittance of channel  $j$  for frequency  $i$ , as seen from the junction, can be expressed as

$$y_{ij} = \frac{1 - \Gamma_{ij}}{1 + \Gamma_{ij}} \quad (7)$$

To eliminate inter-channel interference, we must compensate the reactive component for each frequency by zeroing the junction susceptance,

$$Im \left\{ \sum_j y_{ij} + y_{stbi} \right\} = \sum_j b_{ij} + b_{stbi} = 0 \quad (8)$$

where  $y_{stbi}$  is the admittance of the common stub, connected at the system junction at the frequency of channel  $i$ , and  $b_{stbi}$  is its susceptance part. By equating the susceptance of each channel to zero, the junction is matched for all channels. Assuming a three channels system, we obtain the following

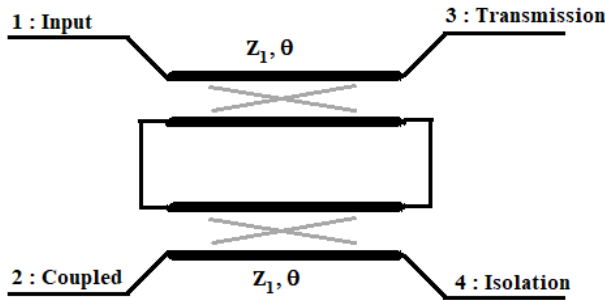


FIGURE 3. 3 DB Tandem hybrid directional coupler.

set of equations,

$$\begin{aligned}
 b_{12}(C_2) + b_{13}(C_3) + b_{stb1} &= 0 \\
 b_{21}(C_1) + b_{23}(C_3) + b_{stb2} &= 0 \\
 b_{31}(C_1) + b_{32}(C_2) + b_{stb3} &= 0
 \end{aligned} \tag{9}$$

where  $C_i$  is the capacitance of channel  $i$  of the coupler. This equation set can be solved only numerically. The solution provides the values for the  $2 \times 3$  varactor capacitors, with a capacitance in the range of 0.5 - 500 pF. Since the optional stub is not connected in the present configuration,  $b_{stbi} = 0$ .

**C. DIRECTIONAL COUPLER**

A 3 dB hybrid directional coupler was designed using the Tandem structure [15], as shown in Fig. 3.

The Tandem structure was chosen, over the simple one, due to its ability to achieve a high coupling factor by using a combination of two couplers with a low coupling factor. This property, of low coupling, improves the accuracy and the simplicity of production of the Tandem coupler over the simple one. To operate efficiently at the higher frequency range of cellular communication, the two internal couplers were designed using broad-side strip-line technology. Rather than using micro-strips, as was done at lower frequencies, we implemented a strip-line configuration, which allows for a full TEM mode [16].

The internal structure of the coupler is shown in Fig. 4. It is built from three layers of dielectric material (Rogers RT5880) encompassing the metal port plates. The spacing between the ground plates is  $B = 0.86$  mm, the spacing between the port plates is  $S = 0.19$  mm, their width is  $W = 0.77$  mm, and their length is  $L = 7.15$  mm. The technical requirements were a bandwidth of 0.8 to 2.5 GHz, a center frequency phase of  $90^\circ$ , a transfer coefficient  $S_{13}$  below  $-2$  dB, and a coupling coefficient  $S_{12}$  larger than  $-5$  dB.

A significant improvement in the performance of the coupler was achieved by constructing the broad-side strip line out of 9 cascaded sections, as shown in Fig. 5. The sections differ from each other by the horizontal offset between the coupled lines. The resulting efficient coupler geometry, combining a multi-section broad-side directional coupler, significantly improves the flatness of the coupler and, consequently, reduces power losses of the system at the edges of the bandwidth [17].

The coupler was designed and simulated with the CST Microwave Studio software. Simulation results of the various

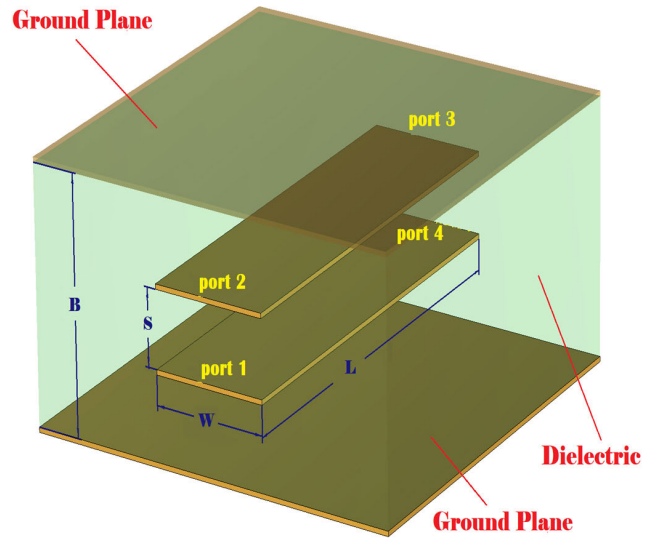


FIGURE 4. Section of a broad-side strip-line coupler.

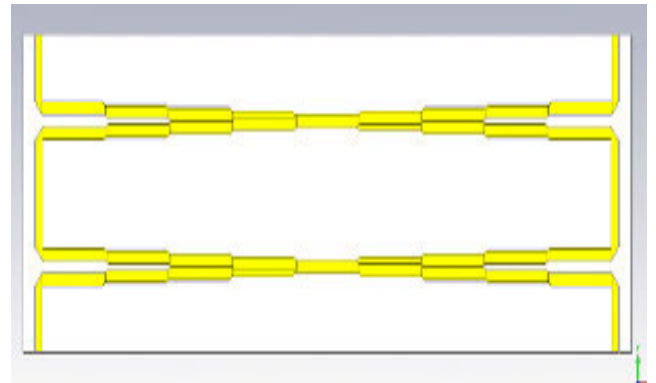


FIGURE 5. Coupler layout design.

S parameters, as a function of frequency, are shown in Fig. 6. The two vertical lines mark the limits of the required frequency range, between 0.8 and 2.5 GHz. In this range, the transmission and coupling coefficients,  $S_{21}$  and  $S_{31}$ , vary between  $-4.50$  and  $-1.92$  dB.

The results of the measurements of the S parameters, performed on the implemented coupler, are shown in Fig. 7. As seen, the performance of the coupler meets the set requirements.

The difference between the simulated results to the measured results is seen in Fig. 8. The measured results agree well with the simulations. The difference between the transmission and coupling curves is small, about 0.7 dB, and is practically insignificant. The larger difference between the loss and isolation curves has no practical implications since it is between 2% to 0.3%.

**D. PHASE SHIFTER**

The phase shifter is composed of a coupler and two varactor banks. Fig. 9 shows the schematics of the phase shifter used for the CST simulations.

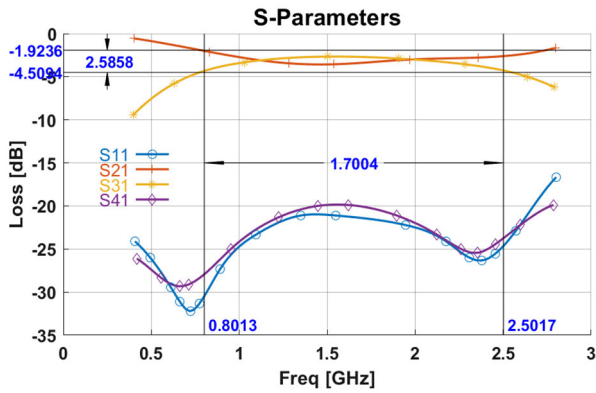


FIGURE 6. Simulations of coupler S parameters spectrum.

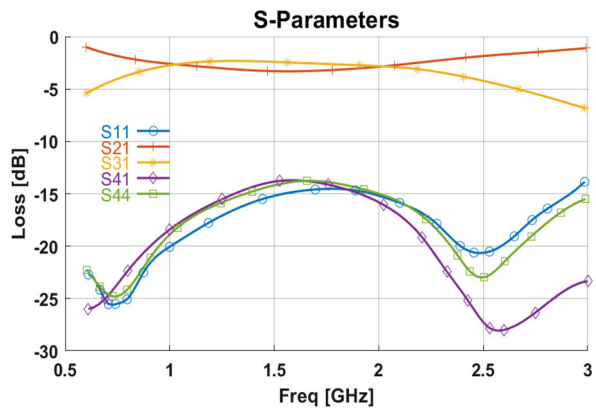


FIGURE 7. Measured S parameters spectrum of the coupler.

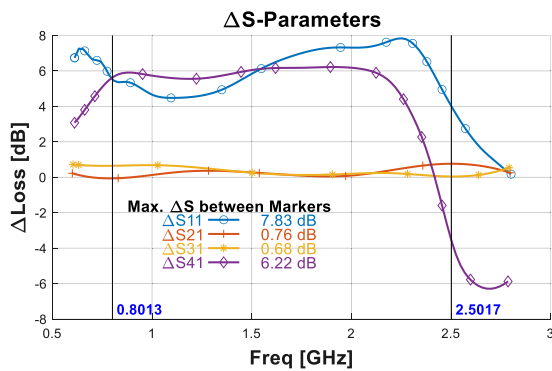


FIGURE 8. Difference between simulated and measured S parameters spectrum of the coupler.

Varactors are used to determine the desired phase shift from port 1 to port 2, which must have a span of  $180^\circ$ . To find the required capacitances, we simulated the phase as a function of frequency for several capacitance values, as shown in Fig. 10. To obtain the entire  $180^\circ$  range, a capacitance range of 0.5 pF to 50 pF is required.

### III. SYSTEM MEASUREMENT RESULTS

To verify the theory and simulations, a system of three channels, operating at three different frequencies, was built and tested. The configuration of the system is shown in Fig. 11.

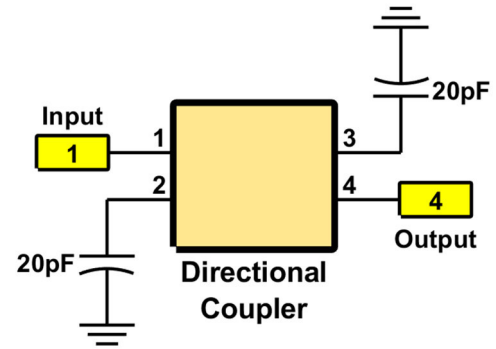


FIGURE 9. Phase shifter schematic for CST.

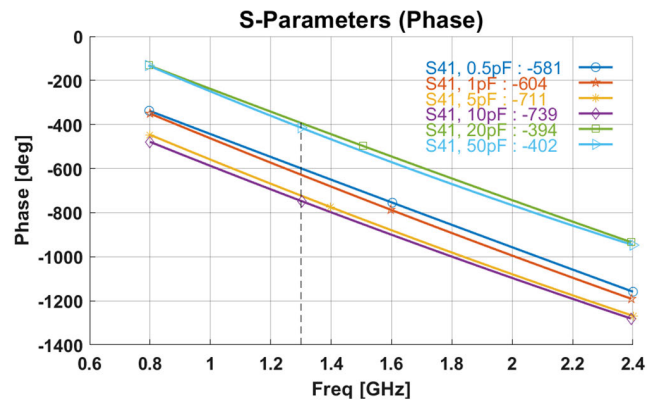


FIGURE 10. Simulation of phase shift vs. frequency for several capacitances.

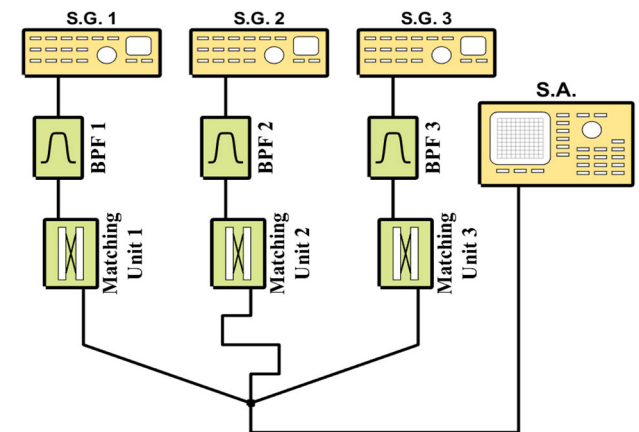
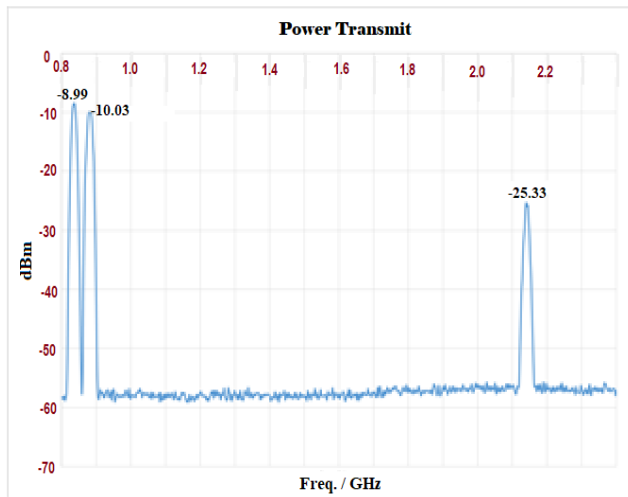


FIGURE 11. System configuration.

The system frequencies were:  $f_1 = 836\text{MHz}$  with a bandwidth of 20 MHz,  $f_2 = 881\text{MHz}$  with a bandwidth of 20 MHz, and  $f_3 = 2140\text{MHz}$  with a bandwidth of 60 MHz. Each channel comprises a signal generator, transmitting one single CW signal into a narrow band filter that enables reception of a single channel frequency and rejects the other two. The output of the narrow BPF is connected to a matching unit, which is a phase shifter with a properly corrected varactor's capacitance value.

The initial capacitances were determined by the numerical solution of equation (4). However, the experimental system has additional losses and unknown parasitic capacitance and



**FIGURE 12.** Untuned system transmitted signals at antenna output without tuning varactors.

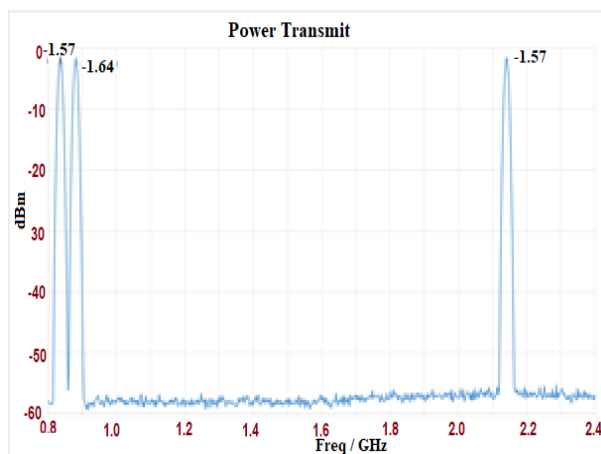


**FIGURE 13.** Tuned system transmitted signals at antenna output with tuned varactor capacitance.

inductance values, which were not included in the simulations. Therefore, the various capacitances were adjusted experimentally to their optimal values.

As a first step, the insertion loss of the system without capacitors was measured to compare the performance of the tuned system to the untuned one. The significant losses for this case, due to 0 dBm transmitted signals at the inputs of the matching units, are shown in Fig. 12. The measured insertion loss at the various frequencies of the three channels was I.L =  $-8.99$  dB at 836 MHz, I.L =  $-10.03$  dB at 881 MHz, and I.L =  $-25.33$  dB at 2140 MHz.

After tuning the system and finding the optimal capacitance values, we obtained the spectrum of the transmitted signals at the output of the antenna, as shown in Fig. 13. The measured values are I.L =  $-1.57$  dB at 836 MHz, I.L =  $-1.64$  dB at 881 MHz, and I.L =  $-1.57$  dB at 2140 MHz.

As can be seen in the figure, a significant improvement in the insertion loss was achieved, from a level of  $-25 \div -9$  dB to  $-1.5$  dB only. These experimental results compare very well with reported performance of switchable tunable BPF

114320

[18], even though our system has a much wider frequency range. In the system reported by Lu et al. the frequency range is limited to 1.134 – 1.235 GHz, as compared to 0.8 – 2.4 GHz in the present system, while their input loss is 2.0 dB.

#### IV. CONCLUSION

We have introduced a technology by which it is possible to reduce the number of antennas in a multi-channel cellular platform. The key component of the system is a dynamic matching unit that was designed, assembled, and measured. A three-channel system prototype was measured and showed an improvement in the insertion loss from a level of  $-25 \div -9$  dB for the untuned system to a level of only  $-1.5$  dB for the tuned one.

The system was tested in field experiments by a commercial company. Three communication methods were tested: a voice channel in a 3G cellular channel, a 4G channel, and a Wi-Fi channel – which indicates a channel bandwidth of 100MHz. The measurement was done by connecting a signal source to the antenna port and checking the signal at one of the system's receiving ports. All the channels operated simultaneously with continuous, high-quality communication throughout the experiment.

We have shown that the tunable multi-coupler method is an efficient technology for combining several transmitters, operating at different frequencies, to a single antenna at the cellular frequency band, transmitting various communication methods.

#### ACKNOWLEDGMENT

This work was partially supported by the Israel Innovation Authority, Meimad program. (Eran Rosenberg and Yoav Koral contributed equally to this work.)

#### REFERENCES

- [1] T. Yang and G. M. Rebeiz, "A 1.26–3.3 GHz tunable triplexer with compact size and constant bandwidth," *IEEE Microw. Wireless Compon. Lett.*, vol. 26, no. 10, pp. 786–788, Oct. 2016.
- [2] C. Zhu, J. Xu, W. Kang, and W. Wu, "Design of balun-integrated switchable low-pass-bandpass triplexer," *IEEE Microw. Wireless Compon. Lett.*, vol. 27, no. 4, pp. 353–355, Apr. 2017.
- [3] J. Dong, Y. Liu, Z. Yang, H. Peng, and T. Yang, "Broadband millimeter-wave power combiner using compact SIW to waveguide transition," *IEEE Microw. Wireless Compon. Lett.*, vol. 25, no. 9, pp. 567–569, Sep. 2015.
- [4] M. L. Laurenzi, Y. M. M. Antar, A. P. Freundorfer, M. Clénet, and S. Jovic, "Miniaturized dual-band power splitter in LTCC for GNSS applications," *IEEE Microw. Wireless Compon. Lett.*, vol. 31, no. 11, pp. 1187–1190, Nov. 2021.
- [5] M. Mizrahi, E. Glassner, N. Bachar, E. Farber, A. Abramovich, and Y. Koral, "VHF multi-channel coupler for RF communication," in *Proc. IEEE Int. Conf. Microw., Commun., Antennas Electron. Syst.*, Nov. 2009, pp. 1–4.
- [6] E. Holdengreber, M. Mizrahi, and E. Farber, "Quasi-dynamical multi-channel coupler based on high temperature superconducting films," in *Proc. IEEE 27th Conv. Electr. Electron. Eng. Isr.*, Nov. 2012, pp. 1–4.
- [7] E. Holdengreber, M. Mizrahi, E. Glassner, Y. Koral, S. E. Schacham, and E. Farber, "Phase shift combiner for multi-channel VHF communication," *Int. J. Microw. Wireless Technol.*, vol. 9, no. 1, pp. 79–83, Feb. 2017.
- [8] E. Holdengreber, M. Mizrahi, E. Glassner, Y. Dahan, H. Castro, and E. Farber, "Design and implementation of an RF coupler based on YBCO superconducting films," *IEEE Trans. Appl. Supercond.*, vol. 25, no. 2, pp. 1–5, Apr. 2015.
- [9] Y. Dahan, E. Holdengreber, M. Mizrahi, S. E. Schacham, and E. Farber, "Multichannel transmitting system based on high-temperature superconducting phase shifter," *IEEE Trans. Appl. Supercond.*, vol. 30, no. 8, pp. 1–6, Dec. 2020.

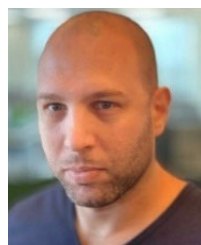
- [10] Y. Dahan, E. Holdengreber, E. Glassner, O. Sorkin, S. E. Schacham, and E. Farber, "Measurement of electrical properties of superconducting YBCO thin films in the VHF range," *Materials*, vol. 14, no. 12, p. 3360, Jun. 2021.
- [11] S. An, B. Zheng, H. Tang, H. Li, L. Zhou, Y. Dong, M. Haerinia, and H. Zhang, "Ultrawideband Schiffman phase shifter designed with deep neural networks," *IEEE Trans. Microw. Theory Techn.*, vol. 70, no. 11, pp. 4694–4705, Nov. 2022.
- [12] S. Fouladi, F. Huang, W. D. Yan, and R. Mansour, "Comblin tunable bandpass filter using RF-MEMS switched capacitor bank," in *IEEE MTT-S Int. Microw. Symp. Dig.*, Jun. 2012, pp. 1–3.
- [13] C. Gijón, M. Toril, M. Solera, S. Luna-Ramírez, and L. R. Jiménez, "Encrypted traffic classification based on unsupervised learning in cellular radio access networks," *IEEE Access*, vol. 8, pp. 167252–167263, 2020.
- [14] E. G. Cristal and L. Young, "Theory and tables of optimum symmetrical TEM-mode coupled-transmission-line directional couplers," *IEEE Trans. Microw. Theory Techn.*, vol. MTT-13, no. 5, pp. 544–558, Sep. 1965.
- [15] R. E. Collin, *Foundations of Microwave Engineering*, 2nd ed. Hoboken, NJ, USA: Wiley, 2001, ch. 3, pp. 170–175.
- [16] D. M. Pozar, *Microwave Engineering*, 3rd ed. Hoboken, NJ, USA: Wiley, 2005, ch. 1, pp. 18–19.
- [17] O. Sorkin, E. Holdengreber, M. Averbukh, S. E. Schacham, and E. Farber, "Directivity enhancement of tight couplers," in *Proc. IEEE Int. Conf. Microw., Antennas, Commun. Electron. Syst. (COMCAS)*, Nov. 2019, pp. 1–5.
- [18] D. Lu, X. Tang, N. S. Barker, and Y. Feng, "Single-band and switchable dual-/single-band tunable BPFs with predefined tuning range, bandwidth, and selectivity," *IEEE Trans. Microw. Theory Techn.*, vol. 66, no. 3, pp. 1215–1227, Mar. 2018.



**MOSHE MIZRACHI** received the B.Sc. and M.Sc. degrees in electrical and electronic engineering from Ariel University. His research interests include designing microwave passive circuits based on superconducting materials and super-resolved sensing for RADAR applications.



**DORON SOLOMON** received the B.Sc. degree in physics and mathematics and the M.Sc. degree in physics from Bar Ilan University. He is currently pursuing the Ph.D. degree in electrical and electronic engineering with Ariel University. He has been in the field of communication research and design, since 1988. In 2003, he co-founded ASOCS Ltd. as the CTO. He also serves as a Chip System Architect Expert with RAD Data Communications Ltd. He was a Leading Algorithm Engineer and a Chip Solution Designer with Tadiran SpectraLink and Innovave. He has extensive experience in the field of software and communication, being a pioneer in the development of a unique heterogeneous SDR architectural design.



**ERAN ROSENBERG** received the B.A. degree in physics from the Technion—Israel Institute of Technology, in 2007. From 2007 to 2016, he was with RAFAEL as an RF Engineer, specializing in electromagnetic simulations and antenna design. In 2016, he joined the high-tech industry. He is currently the Leader of the Antenna and Electromagnetic Team, at the startup Nexite.



**ELDAD HOLDENGREBER** received the Ph.D. degree in electrical and electronic engineering from Ariel University, in 2018. In 2019, he joined the Department of Mechanical Engineering and Mechatronics, Ariel University, as a Faculty Member. He specializes in combining superconductors with advanced THz and RF communication. His research interests include designing superconducting microwave circuits, antenna design, intuitive cognition sensing, and THz detectors based on high TC Josephson junctions.



**YOAV KORÁL** received the B.Sc. and M.Sc. degrees in electrical and electronic engineering from Tel-Aviv University, in 1982 and 1990, respectively. Since 1982, he has been with the Elbit/Elisra Electronic Systems Company, as a Research and Development Engineer, specializing in RF and microwave along with control. Since 2022, he has been with the Department of Electrical and Electronic Engineering, Ariel University, specializing in the field of quantum electronics.



**SHMUEL E. SCHACHAM** received the M.Sc. degree in physics from Bar Ilan University, and the Ph.D. degree from Northwestern University. Currently, he is the Dean of Students at Ariel University. He is also the Founder of the Department of Electrical and Electronic Engineering, Ariel University, where he was the Dean of Engineering for 14 years. His research interests include microelectronics, infrared detectors, quantum electronics, and superconductivity.



**ACHIMEIR MEKEYESS** received the B.Sc. degree in electrical and electronic engineering from Ariel University, in 2014. In 2014, he joined IAI-Elta RADAR System Company and later various startup companies, working as a research and development engineer, specializing in RF, image processing, and digital design.



**ELIYAHU FARBER** received the M.Sc. degree in electrical engineering and the Ph.D. degree in physics from Tel-Aviv University, in 1997 and 2001, respectively. In 2002, he joined as a Faculty Member of the Department of Electrical and Electronic Engineering, Ariel University where he is currently the Chairperson. He is also the Head of the Laboratory for Superconductivity and Optical/Microwave Spectroscopy. His research interests include RF/microwave devices, frequency sources in the terahertz region, antennas, imaging and spectroscopy, novel microwave and IR materials, high-temperature superconducting electronics, and quantum electronics, including Q-bit fabrication.